Revista Ibero-Americana de Humanidades, Ciências e Educação — REASE

doi.org/10.51891/rease.v12i11.31055

SECAGEM POR ATOMIZAÇÃO E LIOFILIZAÇÃO DE LEITE INTEGRAL SEM ADITIVOS: CARACTERÍSTICAS FÍSICO-QUÍMICAS, TECNO-FUNCIONAIS, DE FLUXO E MORFOLÓGICAS DOS PÓS, E EFICIÊNCIA DO PROCESSO

SPRAY- AND FREEZE-DRYING OF ADDITIVE-FREE WHOLE MILK: PHYSICOCHEMICAL, TECHNO-FUNCTIONAL, FLOW, AND MORPHOLOGICAL CHARACTERISTICS OF POWDERS, AND PROCESS EFFICIENCY

SECADO POR ATOMIZACIÓN Y LIOFILIZACIÓN DE LECHE ENTERA SIN ADITIVOS: CARACTERÍSTICAS FISICOQUÍMICAS, TECNOFUNCIONALES, DE FLUJO Y MORFOLÓGICAS DE LOS POLVOS, Y EFICIENCIA DEL PROCESO

Jhonatan Faria Costa[1]
José Roberto Miranda Júnior[2]
Bruna Mara Aparecida de Carvalho Mesquita[3]
Moyses Naves de Moraes[4]
César Augusto Sodré da Silva[5]
Eduardo Basílio de Oliveira[6]
Jane Sélia dos Reis Coimbra[7]

RESUMO: Este estudo avaliou os efeitos da secagem por atomização e da liofilização em leite integral em pó, sem aditivos, quanto às propriedades físico-químicas, cor, características tecno-funcionais, escoamento, morfologia e eficiência do processo. Três lotes independentes de leite foram processados sob quatro condições de secagem por atomização, definidas pela temperatura do ar de entrada (130 e 180 °C) e pela vazão de alimentação (0,2 e 0,8 kg/h); uma condição de liofilização foi utilizada para fins de comparação. Os pós obtidos por atomização apresentaram menor umidade e atividade de água do que o pó liofilizado, indicando maior eficiência na remoção de água e melhor estabilidade durante o armazenamento nas condições avaliadas. Além disso, apresentaram partículas esféricas e mais densas, com uma distribuição de tamanho mais estreita, em contraste com as partículas liofilizadas, que eram irregulares e porosas. Por outro lado, o pó liofilizado apresentou molhabilidade muito mais rápida e melhor fluidez, porém maior higroscopicidade, atividade de água, índice de escurecimento e perdas no processo, sugerindo uma estabilidade físico-química inferior. Entre as condições de secagem por atomização testadas, a de 130 °C/0,8 kg/h proporcionou o melhor equilíbrio geral entre estabilidade e eficiência do processo; contudo, a maior variabilidade na umidade observada para essa condição indica que seriam necessárias réplicas adicionais para confirmar a reprodutibilidade. A condição de 180 °C/0,8 kg/h resultou em uma distribuição de tamanho de partícula mais estreita e menor umidade, mas também prejudicou a molhabilidade e aumentou as perdas de massa.

Palavras-chave: Leite integral em pó. Cinética de desidratação. Propriedades tecno-funcionais.

[1] M.Sc. in Science and Technology of Milk and Dairy Products. D.Sc. student - Universidade Federal de Viçosa (Brazil).
[2] D.Sc. in Food Science and Technology. Postdoc researcher - Universidade Federal de Viçosa (Brazil).
[3] D.Sc. in Food Science and Technology. Professor - Universidade Federal de Minas Gerais, Instituto de Ciências Agrárias (Brazil).
[4] D.Sc. in Food Engineering. Co-adviser - Universidade Federal de Viçosa (Brazil).
[5] D.Sc. in Food Engineering. Professor - Universidade Federal de Viçosa (Brazil).
[6] D.Sc. en Procédés Biotechnologiques et Alimentaires. Co-adviser - Universidade Federal de Viçosa (Brazil).
[7] D.Sc. in Food Engineering. Adviser - Universidade Federal de Viçosa (Brazil).

ABSTRACT: This study evaluated the effects of spray drying and freeze drying on additive-free whole milk powder in terms of physicochemical, color, techno-functional, flow, morphological, and process-efficiency properties. Three independent milk batches were processed under four spray-drying conditions defined by inlet air temperature (130 and 180 °C) and feed flow rate (0.2 and 0.8 kg/h), and one freeze-drying condition was used for comparison. Spray-dried powders showed lower moisture and water activity than freeze-dried powder, indicating greater water-removal efficiency and storage stability under the conditions evaluated. They also exhibited spherical, denser particles and narrower size distributions than the irregular, porous freeze-dried particles. In contrast, freeze-dried powder showed much faster wettability and better flowability, but also higher hygroscopicity, water activity, browning index, and drying losses, suggesting lower physicochemical stability. Among the spray-drying conditions tested, 130 °C/0.8 kg/h provided the best overall balance between stability and process efficiency, although the higher moisture variability observed for this condition indicates that additional replicates would be needed to confirm reproducibility. The 180 °C/0.8 kg/h condition produced a narrower particle-size distribution and lower moisture, but it also impaired wettability and increased mass losses.

Keywords: Whole milk poder. Dehydration kinetics. Techno-functional properties.

RESUMEN: Este estudio evaluó los efectos del secado por atomización y la liofilización en leche entera en polvo sin aditivos, analizando sus propiedades fisicoquímicas, color, características tecno-funcionales, fluidez, morfología y eficiencia del proceso. Se procesaron tres lotes independientes de leche bajo cuatro condiciones de secado por atomización, definidas por la temperatura del aire de entrada (130 y 180 °C) y el caudal de alimentación (0,2 y 0,8 kg/h); asimismo, se utilizó una condición de liofilización a modo de comparación. Los polvos obtenidos mediante secado por atomización presentaron una menor humedad y actividad de agua que el polvo liofilizado, lo que indica una mayor eficiencia en la eliminación de agua y una mejor estabilidad durante el almacenamiento bajo las condiciones evaluadas. Además, mostraron partículas esféricas y más densas, con una distribución de tamaño más estrecha, a diferencia de las partículas liofilizadas, que resultaron ser irregulares y porosas. Por el contrario, el polvo liofilizado presentó una humectabilidad mucho más rápida y una mejor fluidez, pero también una mayor higroscopicidad, actividad de agua, índice de pardeamiento y pérdidas durante el secado, lo que sugiere una menor estabilidad fisicoquímica. Entre las condiciones de secado por atomización probadas, la de 130 °C/0,8 kg/h ofreció el mejor equilibrio general entre estabilidad y eficiencia del proceso; no obstante, la mayor variabilidad en la humedad observada en esta condición indica que serían necesarias réplicas adicionales para confirmar su reproducibilidad. La condición de 180 °C/0,8 kg/h dio lugar a una distribución de tamaño de partícula más estrecha y a una menor humedad, pero también afectó negativamente a la humectabilidad y aumentó las pérdidas de masa.

Palabras clave: Leche entera en polvo. Cinética de deshidratación. Propiedades tecnofuncionales.

1. INTRODUCTION

Powdered milk has high nutritional and economic relevance, with long shelf life, functional properties, broad applications, and reduced transport/storage costs (Farag et al., 2022; O'Sullivan et al., 2019). The most commonly used milk-drying methods include spray drying, tray drying, and freeze drying. Spray drying is the dominant industrial process: concentrated milk is atomized into fine droplets and dehydrated by hot air, minimizing thermal damage due to large surface area and brief heat exposure (Kilic-Akyilmaz et al., 2022; Moejes & Van Boxtel, 2017), though it can cause protein denaturation, lipid oxidation, and loss of heat-sensitive

compounds (Liu et al., 2020). Freeze drying removes water by sublimation under vacuum at low temperature, better preserving sensitive components at a higher energy cost (Zafisah et al., 2017) and retaining native milk proteins and bioactive compounds (Zhou et al., 2025).

Processing parameters (temperature and time) during concentration and drying govern powder quality (moisture, color, particle size, rehydration) (Fialho et al., 2018). Previous studies addressed: surface composition and wetting of spray-dried (SD) milk (Kim et al., 2002); porosity, density, flowability, and wettability of SD and freeze-dried (FD) camel milk (Deshwal et al., 2020); dynamic light scattering (DLS) to evaluate infant formula (growing-up milk) cohesivity (Nugroho et al., 2021); expanded hollow particles at higher temperatures (Felfoul et al., 2022); and smaller, narrower SD particle size distributions vs. FD (Paula et al., 2023; Zhou et al., 2025). However, few studies combined physicochemical, color, flow, and morphological properties with process efficiency under a controlled factorial design, especially for additive-free whole milk.

This study compared spray and freeze drying for additive-free, pasteurized, homogenized whole cow milk (AFW-milk) powder. Unlike commercial powders (which contain emulsifiers, anti-caking agents, or stabilizers), the additive-free formulation isolates processing effects. Thus, the objectives of this study were: (i) to evaluate inlet air temperature (130, 180 °C) and feed flow rate (0.2, 0.8 kg/h), using a factorial design, regarding the physicochemical, color, techno-functional, flow, and morphological properties of the spray-dried (SD) powder, as well as process efficiency (mass loss and retention); (ii) to compare these results with powder obtained via freeze-drying (FD) under defined conditions: freezing at –25 °C for 24 h, followed by freeze-drying at a condenser temperature of –40 °C and 0.1–1.0 mbar for 48 h; (iii) to relate water activity and wettability to morphology using scanning electron microscopy (SEM); and (iv) to discuss the higher browning index of the freeze-dried (FD) powder in relation to cryoconcentration and Maillard reaction dynamics, a hypothesis that was not confirmed in this study but is suggested for future investigation using Maillard markers (e.g., furosine, 5-hydroxymethylfurfural). The results are expected to broaden the understanding of drying-induced changes and support process optimization at the bench scale.

2. MATERIALS AND METHODS

2.1 Milk samples

Three independent batches (replicates) of pasteurized bovine milk (AFW) were obtained from a local dairy processing plant (Viçosa, Minas Gerais, Brazil) between January and August 2025. No processing aids, such as stabilizers, were added to the milk batches in order to determine the intrinsic effects of the heat treatments. The raw milk was characterized for soluble solids (refractometry), total solids and moisture (gravimetric oven drying at 105 °C), lactose (ion chromatography with pulsed amperometric detection), ash (gravimetric incineration), fat (Gerber method), and protein (Micro-Kjeldahl, N × 6.38).

2.2 Milk concentration

Each AFW-milk batch was vacuum-concentrated in a rotary evaporator (Fisatom, Model 810) coupled to a thermostatic bath (Solab, SL-153) at 60 °C, 0.08 MPa (Marconi, MA-058), and 50 rpm. Evaporation was stopped when the concentrate reached 38 °Brix, measured at 25 °C using a refractometer (Instrutherm, RT-60 ATC). Evaporation took 40 to 60 minutes per batch of approximately 1.3 kg. The concentrate was immediately divided into five aliquots randomly assigned to five drying treatments: one freeze-drying and four spray-drying conditions (130–180 °C × 0.2–0.8 kg/h). Samples were refrigerated at 4 °C and processed within 24 h to minimize compositional variation within batches. The proximate composition of the concentrate was determined.

2.3 Spray drying

Concentrated AFW-milk was spray-dried in a bench-scale unit (Büchi Mini Spray Dryer B-290, Switzerland) coupled to a dehumidifier (Büchi B-296, Switzerland) and an air compressor (Schulz MSV6, Brazil). Dehumidified air (Dehumidifier B-296, Switzerland) was used throughout. The equipment operated with an atomizing air flow of 473 L/h, a drying air (aspiration) flow of 35 m^3/h, and a two-fluid nozzle with a 0.7 mm diameter. We varied two factors in a factorial design: inlet air temperature (130 and 180 °C) and feed flow rate (0.2 and 0.8 kg/h). These levels were selected to represent moderate and high drying conditions, based on literature reporting significant differences in milk powder properties within this range

(Felfoul et al., 2022; Zhou et al., 2025), and to remain within the equipment's operating limits (maximum feed rate of up to 2.0 kg/h for aqueous solutions). We applied each of the four conditions to each of the three milk batches (n = 3), with run order randomized. We monitored outlet air temperature continuously and reported it as a response variable for each condition. In each run, approximately 800 g of concentrate were processed over a period of 60 to 240 min. The powder was collected in separate containers for the cyclone and the drying chamber to evaluate process efficiency.

2.4 Freeze drying

For each batch, approximately 200 g of concentrated milk was poured into stainless steel plates (180 mm in diameter, 10 mm in depth) and frozen at -25°C for 24 h in a freezer (GE, Double Integration). As the freezing process was static and slow, ice crystals grew, creating a coarse pore network in the final powder, a characteristic relevant to the wettability and morphology results. The frozen samples were then freeze-dried (Terroni LS3000, Brazil) at a condenser temperature of -40°C and an operating pressure range of 0.1–1.0 mbar for 48 h, yielding freeze-dried (FD) AFW milk powder. The freeze-dryer operated with a single programmed cycle (condenser at –40 °C; chamber pressure 0.1-1.0 mbar; 48 h), without independent control of primary (sublimation) and secondary (desorption) drying stages. Drying completion was defined by the fixed 48 h cycle, and no re-freezing step was performed between stages. The absence of real-time product temperature or mass-loss monitoring to confirm the endpoint is acknowledged as a limitation. The freeze-dried powder was weighed, placed in sealed polyethylene containers, wrapped in aluminum/PVC film to prevent light and moisture exposure, and stored at 4°C. Analyses were performed between 1 and 5 days after processing, as water activity and browning can change during this period.

2.5 Proximate composition and water activity of AFW-milk powder

Proximate composition was determined in triplicate according to AOAC (2016) methods. Moisture and total solids were determined gravimetrically by oven drying at 100 ± 5.0 °C to constant mass (AOAC 927.05); crude protein by the Micro-Kjeldahl method (AOAC 991.20), using a nitrogen-to-protein conversion factor of 6.38; fat by the Gerber method (AOAC

2000.18), after reconstituting the powder in water at 25 ± 0.2°C; and ash by gravimetric incineration (AOAC 930.30). Results are expressed in g/100 g of powder (wet basis).

Lactose was quantified (Suess, 2021) by ion chromatography with pulsed amperometric detection (Metrohm 850 Professional IC) on a Metrosep Carb 2 column (150/4.0 mm, 30 °C), using 100 mM NaOH at 0.5 mL/min, a 20 μL injection volume, and a 30-min run time. Powder samples were extracted in water at 50 °C, diluted, and filtered through a 0.22 μm PVDF membrane. Quantification relied on an external calibration curve (five levels, 1.0–100.0 mg/L; $R^2 > 0.999$). The limit of detection (LOD) and limit of quantification (LOQ) were 0.3 and 0.9 mg/L, respectively, estimated based on signal-to-noise ratios of 3:1 and 10:1.

Water activity was measured at 25 °C and ambient pressure using the dew point method with an AquaLab PRE analyzer (Meter Group, USA) (AOAC 978.18).

2.6 Colorimetric analysis

Powder color was measured using a portable colorimeter (Minolta, CR-20 Color Reader, Japan) under CIE standard illuminant D65, following calibration with the instrument's own white reference plate. The CIELAB parameters were recorded: L (lightness, 0 = black to 100 = white), a (+a = redness, –a = greenness), and b (+b = yellowness, –b = blueness). We took three readings for each powder; we packed the sample to a fixed depth in a sample container with a leveled surface.

The browning index (BI) was calculated from the CIELAB coordinates, according to Nasser et al. (2017):

$$Browning\ index\ (BI) = \frac{[100 * (x - 0.31)]}{0.17} \quad (1)$$

$$x = \frac{[a + (1.75 * L)]}{(5.645 * L) + a - (3.012 * b)} \quad (2)$$

Where L, a, and b are the measured CIELAB values. BI quantifies brown color intensity derived from the color coordinates. Although it is commonly used as an indirect indicator of browning reactions, it does not, by itself, identify the responsible mechanism.

2.7 Techno-functional properties of AFW-milk powder

2.7.1 Wettability

Wettability is defined as the time required for powder particles to become completely wetted upon placement on the water surface; it was determined following the procedure described in standard ISO/TS 17758:2014 (IDF/RM 87:2014), adapted as described below. Wettability was determined following the principle of ISO/TS 17758:2014 (IDF/RM 87:2014), adapted for non-instant powders, since the standard was originally developed for instant milk powder. A 10.0 g powder sample was poured from a fixed height of approximately 10 cm, through a funnel, onto the surface of 250 g of deionized water at 25 °C. A stopwatch recorded the time from the powder's initial contact with the water surface until all particles were completely submerged (with no dry particles remaining on the surface). Measurements were performed in triplicate for each powder.

2.7.2 Dispersibility

Dispersibility was determined following ISO/TS 17758:2014 (IDF/RM 87:2014), adapted from Hamedi et al. (2021). A 10 g powder sample (w1) was weighed in a centrifuge tube and dispersed in 100 g of deionized water at 25 ± 0.5 °C (w0). The suspension was manually agitated for 1 min (60 complete up-and-down movements at approximately 1 movement/s) and allowed to stand for 5 min. The suspension was then poured over a sieve with a 150 μm aperture. The total solids content of the filtrate (TSf) was determined gravimetrically (AOAC 927.05), and dispersibility was calculated as:

$$Dispersibility\ (\%) = \frac{(w0 + w1) * TSf\ (\%)}{w1 * (\frac{100 - M\ (\%)}{100})} \quad (3)$$

Where w0 = mass of water (g), w1 = mass of the sample (g), tsf = total solids content of the filtrate (%), and M = moisture content of the sample (%). Analyses were performed in triplicate.

2.7.3 Insolubility index

The insolubility index was determined according to ISO 8156:2005 (IDF 129:2005), applicable to whole milk powder. A 13 g test portion of the powder was reconstituted in 100 mL of distilled/demineralized water at 25 ± 0.2 °C using a propeller-type stirrer at 300 rpm for 5 min. Transfer the reconstituted milk to a graduated centrifuge tube (0.1 mL to 50 mL) and centrifuge at 3000g for 5 min (Eppendorf, Centrifuge 5430, Alemanha). The supernatant was removed, the sediment was redispersed in 20 mL of water at 25 ± 0.2 °C, and the mixture was centrifuged again at 3000g for 5 min. The sediment volume was read directly from the graduated tube and expressed in milliliters (mL).

2.7.4 Hygroscopicity

Hygroscopicity was determined following Schuck et al. (2012). Approximately 2 g of powder (w1) was weighed into a 50 mL glass beaker (w0) and placed in a desiccator at 25 ± 0.2 °C, over a saturated NaCl solution (approximately 75% relative humidity), for 7 days under vacuum. After this period, the dish and sample were weighed again (w2), and hygroscopicity was calculated as:

$$Hygroscopicity\ (\%) = \frac{(w2 - w1 - w0) + (w1 * M * 10)}{(w2 - w0) * 10} \quad (4)$$

Where w0 = mass of the Petri dish (g), w1 = initial mass of the sample (g), w2 = final mass of the dish with the sample (g), and M = moisture content of the sample (%). Analyses were performed in triplicate.

2.8 Flow properties of AFW-milk powder

2.8.1 Bulk density and tapped density

The apparent and compacted densities were determined following Pugliese et al. (2017). A 100 mL graduated cylinder was filled with the powder via free flow through a funnel, without compaction, and the excess was leveled off without applying pressure. The mass of powder (w1) required to fill the test tube to 50 mL (apparent volume, Va) was weighed, and the apparent density was calculated as:

$$Apparent\ density\ (g/mL)(Da) = \frac{w1}{Va} \quad (5)$$

The compacted density was obtained using the same method; the graduated cylinder filled to 50 mL was then compacted by tapping. After 100 manual taps and a constant volume was reached, the new volume (Vb) was recorded. The density after compaction was calculated as:

$$Compacted\ density\ (g/mL)(Dc) = \frac{w1}{Vb} \quad (6)$$

Where w1 = mass of the sample (g), Va = apparent volume in the graduated cylinder (ml), and Vb = compacted volume in the graduated cylinder (ml). All measurements were performed in triplicate.

2.8.2 Carr index and Hausner ratio

The fluidity and cohesiveness of the powder were evaluated using the Carr index (compressibility index) and the Hausner ratio, calculated from the apparent and compacted densities, following Juárez-Enríquez et al. (2022) and Pugliese et al. (2017):

$$Carr\ index\ (\%) = \frac{Dc - Da}{Dc} * 100 \quad (7)$$

$$Hausner\ ratio = \frac{Dc}{Da} \quad (8)$$

Where Dc = compacted density (g/ml) and Da = apparent density (g/ml). Both were measured per replicate.

The Carr index reflects the powder's tendency to consolidate under compaction (tapping), with lower values indicating better flowability; the Hausner ratio is a dimensionless measure of flowability and cohesiveness, where values close to 1 indicate free-flowing powders. Flowability was classified according to the ranges described in Table 1 (adapted from JUAREZ-ENRIQUEZ et al., 2022), which classifies the FD powder as having excellent flowability.

Table 1. Classification of powder flow according to the Carr index and Hausner ratio (Adapted from JUAREZ-ENRIQUEZ et al., 2022)

Flow classification	Carr index	Hausner ratio
Excellent	<15%	<1.10
Good	15% < IC < 18%	1.10 < HR < 1.25
Poor	18% < IC < 22%	1.25 < HR < 1.40
Bad	22% < IC < 35%	
Very bad	35% < IC < 40%	
Non-flowing	>40%	>1.40

2.9 Morphological characterization of AFW-milk powder

2.9.1 Particle size analysis (wet method)

Particle size distribution was determined by dynamic light scattering using a Litesizer 500 instrument (Anton Paar, Austria), with isopropanol as the dispersant (refractive index of isopropanol = 1.38; refractive index of milk particles = 1.46). A 0.05 g sample was dispersed in 10 mL of isopropanol and vortex-agitated for 2 min. Measurements were performed in triplicate for each powder.

The Span parameter was calculated to assess the width of the particle size distribution:

$$Span = \frac{d[0.9] - d[0.1]}{d[0.5]} \quad (9)$$

where d[0.1], d[0.5], and d[0.9] are the particle diameters below which 10%, 50%, and 90% of the particles lie, respectively. Lower Span values indicate narrower, more homogeneous distributions, whereas higher values indicate greater polydispersity (Nugroho et al., 2021; Zhou et al., 2025).

Isopropanol was selected following Nugroho, Outinen, Toikkanen, and Rojas (2021). However, as a non-polar solvent, it may partially dissolve surface lipids, potentially altering particle size assessment, particularly when surface fat content differs between spray-dried and freeze-dried samples. This bias is acknowledged as a limitation of the wet dispersion approach; all samples were treated identically to minimize it.

2.9.2 Surface topography

We examined the surface morphology of powder particles from each drying treatment by scanning electron microscopy (SEM). Powder was spread onto metal mounts with double-sided carbon tape, then gold-coated (Quorum Q150R S) under vacuum to improve electrical conductivity and prevent charging. Micrographs were acquired (Zeiss LEO 1430 VP) at 12 kV and magnifications of 200×, 1000×, 2000×, and 4000×, allowing visualization of general morphology and surface details. Three samples per treatment were examined, with images from at least three randomly selected fields per sample; representative micrographs are shown in Figures 1 and 2. Micrographs were used to relate particle morphology (surface roughness, pores, depressions, agglomerates) to differences in wettability, hygroscopicity, and darkening.

2.10 Process efficiency

Process efficiency was expressed as powder yield, drying loss, and powder retention in the drying chamber, calculated from a mass balance for each drying run. For spray drying, total solids fed (concentrate mass × total solids content) and dry powder recovered from the cyclone receiver were weighed. The same equations were applied to freeze drying, using powder recovered from the plates and the total solids of the loaded concentrate. Each run was weighed individually, and the three parameters were reported per condition as mean ± SD (n = 3).

2.10.1 Drying yield

The drying process yield was calculated according to Equation 10:

$$Drying\ \ yield\ (\%) = \frac{wp\ (g) * TSp\ (\%)}{wc\ (g) * TSc\ (\%)} * 100 \quad (10)$$

Where wp = mass of the dried powder (g), tsp = total solids content of the powder (%), wc = mass of the concentrate (g), tsc = total solids content of the concentrate (%).

The mass of the feed concentrate (wc) was determined gravimetrically by weighing the feed reservoir before and after each batch, and the mass of collected powder (wp) was obtained by weighing the powder recovered from the collection vessel and the drying chamber. The total solids content (tsc and tsp) was determined.

2.10.2 Loss during drying

Drying loss, including powder retained in the drying chamber, cyclone, and exhaust lines, plus collection losses, was calculated using Equation 11:

$$Loss\ during\ drying\ (\%) = 100 - Drying\ \ yield\ (\%) \quad (11)$$

2.10.3 Powder retention in the drying chamber

Powder retention in the drying chamber was determined gravimetrically after each spray-drying run, according to Equation 12:

$$Powder\ retention\ \ in\ the\ drying\ chamber\ (\%) = \frac{wdc\ (g)}{wpm\ (g)} * 100 \quad (12)$$

Where wdc is the mass of powder retained in the drying chamber (g), and wpm is the total mass of powder recovered in the test (g), calculated as the sum of the powder collected in the collection vessel (wp) and the powder retained in the drying chamber (wdc). Wdc was determined by carefully weighing the retained powder after cooling to room temperature.

2.11 Statistical analysis

The experiment followed a completely randomized design (CRD) with five treatments and three replicates each (n = 3). Treatments comprised four spray-drying conditions (2 × 2 inlet air temperature × feed flow rate: 130 °C/0.2 kg/h, 130 °C/0.8 kg/h, 180 °C/0.2 kg/h, 180 °C/0.8 kg/h) and one freeze-drying condition (freezing at –25 °C for 24 h, followed by freeze-drying at a condenser temperature of –40 °C and 0.1–1.0 mbar for 48 h).

Data were analyzed by ANOVA. Normality (Shapiro-Wilk) and homogeneity of variances (Levene) were verified. When significant ($p < 0.05$), means were compared by Tukey's test. Comparisons were structured at four levels: (i) among all five treatments; (ii) between processes (spray drying, individual or pooled, vs. freeze-drying); (iii) between spray-drying inlet air temperatures (130 and 180 °C) and the freeze-drying freezing temperature (–40 °C), the latter treated as a freezing parameter, not an equivalent drying temperature; and (iv)

between spray-drying feed flow rates (0.2 vs. 0.8 kg/h). Levels (ii)–(iv) are planned contrasts and are reported as such.

Results are presented as mean ± standard deviation with coefficient of variation (CV%) for each determination. Means that do not differ statistically ($p \geq 0.05$) share the same letter; grouping thus reflects statistical equivalence, not presumed superiority, and no difference is claimed between conditions not found statistically distinguishable. Analyses were performed in R, version 4.6.0.

3. RESULTS AND DISCUSSION

3.1 Proximate composition of AFW-milk and water activity of AFW-milk powders

3.1.1 Proximate composition of AFW-milk and concentrate

The proximate composition of the additive-free raw whole milk (AFW) (mean ± SD, n = 3) was 12.00 ± 0.00 °Brix, 12.09 ± 0.18% total solids, 87.91 ± 0.18% moisture, 5.14 ± 0.25% lactose, 0.67 ± 0.03% ash, 3.00 ± 0.04% fat, and 3.21 ± 0.07% protein. These values match the typical composition of Brazilian whole milk (Brasil, 2018) and confirm that no processing aids or adulterants were added to the batches.

After the concentration step, the concentrate showed 38.67 ± 1.45 °Brix, 36.72 ± 3.62% total solids, 63.28 ± 3.62% moisture, 14.24 ± 2.37% lactose, 2.31 ± 0.15% ash, 10.53 ± 0.20% fat, and 9.75 ± 0.91% protein, corresponding to a concentration factor of approximately 3.0-fold based on total solids. The increase in total solids and the proportional concentration of all components confirm the efficiency of the vacuum evaporation step and the homogeneity of the concentrate used in the drying trials.

Table 2. Effect of different drying processing conditions on the powder characteristics. Data are presented as mean ± standard deviation. Different superscript letters within the same line indicate significant differences ($p < 0.05$) according to Tukey's test.

	Spray drying				Freeze drying	p-value
	130°C/0.2kg/h	130°C/0.8kg/h	180°C/0.2kg/h	180°C/0.8kg/h		
Composition						
Total solids (%)	99.14 ± 0.15 a	98.98 ± 0.53 a	99.32 ± 0.20 a	98.91 ± 0.04 a	94.27 ± 0.48 b	<0.001

Moisture (%)	0.86 ± 0.15 b	1.35 ± 1.01 b	0.68 ± 0.20 b	1.09 ± 0.04 b	5.73 ± 0.48 a	<0.001
Total protein (%)	26.05 ± 0.47	26.36 ± 1.03	25.41 ± 1.06	25.99 ± 0.19	25.07 ± 0.17	0.233
Lipids (%)	26.43 ± 0.51	26.43 ± 0.51	26.57 ± 0.51	26.47 ± 0.40	25.90 ± 1.65	0.883
Lactose (%)	41.23± 3.75	41.46± 5.68	40.33± 0.99	42.01± 5.67	41.08± 4.28	0.993
Ash (%)	5.90 ± 0.09 a	5.80 ± 0.07 a	5.89 ± 0.07 a	5.89 ± 0.07 a	5.50 ± 0.16 b	0.002
Ash (dry basis, %)	5.95 ± 0.08	5.88 ± 0.10	5.93 ± 0.07	5.95 ± 0.07	5.83 ± 0.18	0.647
Water activity	0.219 ± 0.040 b	0.261 ± 0.020 b	0.180 ± 0.050 b	0.160 ± 0.020 c	0.626 ± 0.070 a	<0.001
Color properties						
Luminosity (L*)	63.83 ± 4.81	65.37 ± 5.59	61.93 ± 3.49	64.17 ± 5.10	55.30 ± 5.54	0.178
a*	-1.40 ± 0.17	-1.13 ± 0.25	-1.40 ± 0.61	-1.37 ± 0.32	-1.77 ± 0.77	0.634
b*	12.27 ± 1.07 b	13.00 ± 2.61 b	13.97 ± 0.76 b	12.83 ± 0.58 b	19.63 ± 1.72 a	<0.001
Darkening index	18.91 ± 0.81 b	19.86 ± 3.32 b	23.03 ± 2.91 b	19.98 ± 1.71 b	39.72 ± 4.53 a	<0.001
Physicochemical properties						
Wettability (min)	130.90 ± 0.85 c	107.77 ± 30.27 c	426.57 ± 63.27 a	325.00 ± 15.87 b	37.20 ± 6.72 d	<0.001
Dispersibility (%)	69.60 ± 7.37	68.55 ± 12.49	72.85 ± 11.60	73.34 ± 10.46	50.73 ± 11.18	0.135
Insolubility (%)	0.67 ± 0.29 c	0.37 ± 0.23 c	2.57 ± 0.78 b	0.57 ± 0.12 c	3.60 ± 0.76 a	<0.001
Hygroscopicity (%)	8.60 ± 1.52 b	13.61 ± 9.83 b	7.08 ± 1.86 b	10.85 ± 0.38 b	56.62 ± 4.69 a	<0.001
Flow and density properties						
Apparent density (g/mL)	0.37 ± 0.03 b	0.34 ± 0.02 b	0.21 ± 0.03 c	0.26 ± 0.04 c	0.55 ± 0.06 a	<0.001
Compacted density (g/mL)	0.47 ± 0.04 b	0.41 ± 0.03 b	0.27 ± 0.04 c	0.32 ± 0.06 c	0.61 ± 0.06 a	<0.001
Carr index (%)	19.75 ± 0.94 a	17.84 ± 2.31 b	20.90 ± 0.38 a	17.97 ± 1.86 b	9.28 ± 0.59 c	<0.001
Hausner ratio	1.25 ± 0.02 b	1.21 ± 0.03 b	1.26 ± 0.01 a	1.22 ± 0.03 b	1.10 ± 0.01 c	<0.001
Particle size distribution						
d [4.3] (μm)	0.599 ± 0.070 a	0.683 ± 0.130 a	1.024 ± 0.090 b	0.736 ± 0.080 a	1.074 ± 0.190 b	0.003
d [0.1] (μm)	0.204 ± 0.030 a	0.451 ± 0.090 ab	0.698 ± 0.170 b	0.415 ± 0.070 a	0.235 ± 0.050 a	0.002
d [0.5] (μm)	0.584 ± 0.090 a	0.624 ± 0.090 a	0.941 ± 0.040 b	0.690 ± 0.060 a	1.076 ± 0.140 b	0.001

d [0.9] (μm)	1.102 ± 0.070 b	0.967 ± 0.100 ab	1.329 ± 0.050 c	0.851 ± 0.060 a	2.085 ± 0.150 d	<0.001
Span	1.538 ± 0.190 a	0.827 ± 0.110 b	0.670 ± 0.080 b	0.632 ± 0.070 b	1.720 ± 0.100 a	<0.001
Process efficiency						
Loss during drying (%)	5.10 ± 0.75 a	4.90 ± 0.38 a	9.71 ± 1.52 b	8.60 ± 1.52 b	9.14 ± 0.44 b	<0.001
Retention (drying chamber)	53.63± 0.63 a	38.25± 3.26 c	54.77± 2.09 a	42.99± 0.91 b	NA	<0.001

The proximate composition and water activity of the powders obtained via the four spray-drying (SD) treatments and freeze-drying are presented in Table 2. One-way ANOVA followed by Tukey's HSD test ($p < 0.05$) was applied to the powder data; superscript letters indicate significant differences between treatments.

3.1.2 Water content and water activity of AFW-milk powders

Moisture content and water activity (aw) are presented in Table 2. Spray-dried (SD) powders had lower moisture (1.00 ± 0.52%) and aw (0.205 ± 0.05) than freeze-dried (FD) powder ($p < 0.05$) (5.73 ± 0.48% and 0.626 ± 0.07, respectively), indicating greater water-removal efficiency for SD under the evaluated conditions.

Moisture and aw control key quality changes in milk powder, such as lipid oxidation and shelf life (Phosanam et al., 2021; Ryabova et al., 2023). The lower values for SD powders are linked to rapid evaporation during atomization into heated air, where reduced droplet size increases surface area for heat and mass transfer during the short residence time.

SD powders showed lower moisture (1.00 ± 0.52%) and higher total solids (99.14–99.32%) than FD powder (5.73 ± 0.48% moisture and 94.27 ± 0.48% total solids) (Table 2), corroborating the greater water-removal efficiency of spray drying under the evaluated conditions. The higher residual moisture of the FD powder can be attributed to structural and operational factors inherent to the freeze-drying process. The concentrated milk was frozen slowly at −25 °C for 24 h and dried in layers of 10 mm, which may have favored the formation of a dense surface crust and increased the resistance of the dried layer to water-vapor transport during primary drying (Mass transfer resistance in freeze-drying increases with the thickness of the

dried solid above the sublimation front). Additionally, primary and secondary drying were not controlled separately, and the process was terminated at a fixed time (48 h) without real-time monitoring of product temperature or mass loss, which may have limited bound-water removal during secondary drying. Slow freezing can also produce heterogeneous ice-crystal networks, and the resulting pore structure may not fully facilitate vapor escape, particularly in thicker sample layers. These combined effects are consistent with the higher moisture content and lower total solids observed in FD powder compared with SD powders.

3.1.3 Proximate composition of AFW-milk powders

Freeze-dried (FD) powder showed higher residual moisture (5.73 ± 0.48%) than spray-dried (SD) powders (1.00 ± 0.52%) (Table 2), which directly influenced the expression of ash content on a wet basis. Because the mineral fraction is diluted by the higher water content in the FD powder, its ash content on a wet basis (5.50 ± 0.16%) appeared lower than that of SD powders (5.80 ± 0.07%–5.90 ± 0.09%). However, when expressed on a dry basis, FD ash (5.83 ± 0.18%) was similar to SD ash (5.88 ± 0.10%–5.95 ± 0.08%), as expected for the same milk matrix. One-way ANOVA confirmed no significant effect of drying treatment on ash content ($p = 0.647$), and Tukey's test indicated no significant pairwise differences ($p > 0.05$). Therefore, the apparent difference in ash content on a wet basis reflects the higher moisture content of the FD powder rather than any actual change in mineral content. This behavior highlights the importance of expressing compositional data consistently (wet or dry) when comparing products with different moisture contents (Schuck et al., 2012).

3.2 Colorimetry indices of AFW-milk powders

Color parameters and browning index are presented in Table 2. FD powder showed significantly higher b* and browning index (13.12 ± 1.25) than SD powders (12.92 ± 1.69), indicating a shift toward yellow. In SD samples, this is attributed to lower residual moisture linked to higher inlet air temperature (Felfoul et al., 2022).

The higher browning index and b* of FD powder are noteworthy, since freeze-drying operates under milder thermal conditions than spray drying; this differs from the trend commonly reported for low-temperature drying. As this study did not quantify Maillard reaction markers (e.g., furosine, 5-hydroxymethylfurfural), lactose crystallinity, protein

denaturation, or glass transition temperature (Tg), the mechanisms below are hypotheses to be tested, not established explanations.

The browning behavior of the FD powder may be related to phenomena occurring during the freezing stage, such as cryoconcentration, as described below. Delayed freezing may promote cryoconcentration, in which water freezes selectively and concentrates solutes (lactose, proteins, mineral salts) in unfrozen channels. Balde and Aïder (2017), working with skim milk, reported that during sublimation (primary drying) and desorption (secondary drying), associating these highly concentrated solutes with temperature fluctuations can increase non-enzymatic browning and favor melanoidin formation.

A second factor is increased molecular mobility during secondary drying and/or storage. Residual moisture lowers the glass transition temperature (Tg), the temperature at which an amorphous material transitions from a rigid, glassy state to a viscous, rubbery state, and can promote transition to the rubbery state, even under moderate thermal conditions. Water absorption disrupts intramolecular interactions (e.g., hydrogen bonds between lactose and protein chains) and fosters new interactions with water, reducing matrix rigidity and lowering the glass-to-rubbery transition temperature (Jouppila & Roos, 1994; Li et al., 2016; Roos, 2010). Under these conditions, the Maillard reaction may accelerate, as suggested by literature-based models and predicted by the Williams-Landel-Ferry (WLF) model (Jouppila & Roos, 1994; Pugliese et al., 2018). This mechanism is proposed as a literature-based interpretation of the observed browning behavior.

Despite FD powder's greater susceptibility to browning, freeze-drying remains relevant for high-value-added products; its application to heat-sensitive compounds can justify operating costs and stringent packaging requirements (with effective moisture barriers) to mitigate moisture absorption (Deshwal et al., 2020).

3.3 Techno-functional properties of AFW-milk powders

Reconstitution properties included wettability and dispersibility. Wettability is a liquid's ability to penetrate dry powder particles, representing the initial rehydration step, measured as the time for a powder mass to become fully wetted and sink (Schuck et al., 2012). Dispersibility is the capacity of wetted particles to separate and distribute uniformly without forming agglomerates. Together, they determine how easily milk powder

reconstitutes into a homogeneous liquid (Gaiani et al., 2007; Schuck et al., 2012). Rehydration involves sequential stages of wetting, swelling, dispersion, and dissolution, influenced by surface composition, particle size, and agglomeration (Gaiani et al., 2007).

Hygroscopicity and insolubility are stability-related properties. Hygroscopicity is the powder's ability to adsorb atmospheric moisture at high relative humidity, affecting shelf life, lump formation, and flowability (Braga et al., 2019; Sharma et al., 2012). Insolubility, expressed by the insolubility index, measures sediment volume after reconstitution and centrifugation; high values indicate incomplete dissolution, compromising functional and sensory quality (Fournaise et al., 2020; Sharma et al., 2012).

The wettability time of FD powder (37.20 ± 6.72 min) was notably shorter than that of SD powders (mean of 247.56 ± 142.68 min, ranging from 107.77 to 426.57 min depending on the condition), consistent with the morphological differences observed by SEM (Figures 1 and 2). FD particles exhibited an irregular, porous, and microporous structure (Figure 1-A, 1-D; Figure 2-B) that facilitates capillary water penetration, whereas SD particles had a dense, spherical surface (Figure 1-B, 1-C) that hinders water penetration. Thus, FD wettability was influenced by morphology (larger particles with larger pores) and surface composition, facilitating water penetration into particle pores (Zhou et al., 2025). The porous, microporous structure observed by SEM (Figures 1 and 2) is the primary morphological feature explaining the faster water uptake of FD powder. In contrast, for spray-dried dairy powders, surface-active components such as fat and protein tend to be over-represented at the particle surface, while lactose is depleted (Wu et al., 2014), which may contribute to the lower wettability observed for SD powders.

Inlet air temperature significantly affected wettability during SD: increasing from 130 °C (119.33 ± 22.96 min) to 180 °C (375.78 ± 69.26 min) increased wetting time. This behavior is consistent with the lower bulk and tapped densities at 180 °C (0.21–0.26 and 0.27–0.32 g/mL, respectively) compared to 130 °C (0.34–0.37 and 0.41–0.47 g/mL) (Table 2), indicating a more expanded and porous particle structure that hinders water penetration (Ji et al., 2016; Wu et al., 2014).

Although SD powders showed longer wetting times than FD powder, they also exhibited a lower insolubility index (Table 2). This apparent paradox reflects different

rehydration stages: wettability measures initial liquid penetration, whereas insolubility quantifies undissolved residue after reconstitution and centrifugation (Schuck et al., 2012). The lower insolubility of SD powders indicates that, once wetted, they disperse, leaving less residue; FD powder, despite superior wettability, retained more insoluble material. The mechanisms were not directly characterized; possible factors include differences in particle cohesion and surface composition (Zouari et al., 2020).

In milk powders, amorphous lactose, glass transition temperature (Tg), surface composition, and particle morphology govern hygroscopicity (Jouppila & Roos, 1994; Kim et al., 2002; Li et al., 2016). FD powder hygroscopicity (56.62 ± 4.69%) was substantially higher than that of SD powders (Table 2). This interpretation is based on literature reports. Future studies with direct measurements of lactose crystallinity, Tg, and surface composition could further confirm these mechanisms. First, freeze-drying preserves lactose in a highly hygroscopic amorphous state, whereas high SD temperatures (130–180 °C) can promote lactose crystallization, reducing moisture adsorption (Jouppila & Roos, 1994). Second, FD powder exhibited a porous, irregular morphology (Figure 1), resulting in a larger specific surface area for water vapor adsorption (Zhou et al., 2025), consistent with the higher Span value (1.720 ± 0.10). Third, FD powder's higher residual moisture (5.73 ± 0.48%) and water activity (0.626 ± 0.070) are expected to lower Tg and increase molecular mobility, facilitating moisture absorption (Jouppila & Roos, 1994). Fourth, SD powder surfaces, rich in fat and partially crystalline lactose, tend to form a hydrophobic barrier reducing water adsorption (Kim et al., 2002; Nugroho et al., 2021).

In contrast, the lower hygroscopicity of SD powders reflects their spherical, dense morphology, lower surface area, higher surface crystallinity, and lower residual moisture, which reduce amorphous regions and limit water-vapor diffusion. Lower hygroscopicity in SD powders may reflect differences in morphology, surface composition, and water activity. Thus, SD powders are more stable under humid conditions, whereas FD powder, despite superior reconstitution properties, requires stringent packaging to mitigate moisture uptake (Deshwal et al., 2020).

3.4 Flow properties of AFW-milk powders

Drying methods and process parameters influenced the flow properties of the powders, which were evaluated based on bulk density, tapped density, Carr index, and Hausner ratio.

The freeze-dried (FD) powder exhibited the highest bulk and tapped densities (Table 2), indicating a denser packing structure than that of the spray-dried (SD) powders. Consequently, its Carr index and Hausner ratio were the lowest among the treatments (Table 2), corresponding to an "excellent" flowability classification (Table 1). This behavior was attributed to the uniform structure of the FD powder, which reduces inter-particle cohesion (Juarez-Enriquez et al., 2022).

The SD powders showed lower bulk and tapped densities and higher compressibility and cohesiveness than the FD powder (Table 2), with flowability ranging from good to poor and a greater tendency toward cohesion. This lower density, associated with fine, poorly agglomerated particles, can increase packaging and transportation costs (Deshwal et al., 2020; Pugliese et al., 2017). These flow issues help explain why commercial milk powders often include emulsifiers such as lecithin, which modify surface properties, reduce interparticle cohesion, and improve flowability and dispersibility (Fournaise et al., 2020; Sharma et al., 2012). Lecithin forms a hydrophobic surface layer that reduces moisture adsorption and liquid-bridge formation between particles, mitigating caking and improving long-term flow stability.

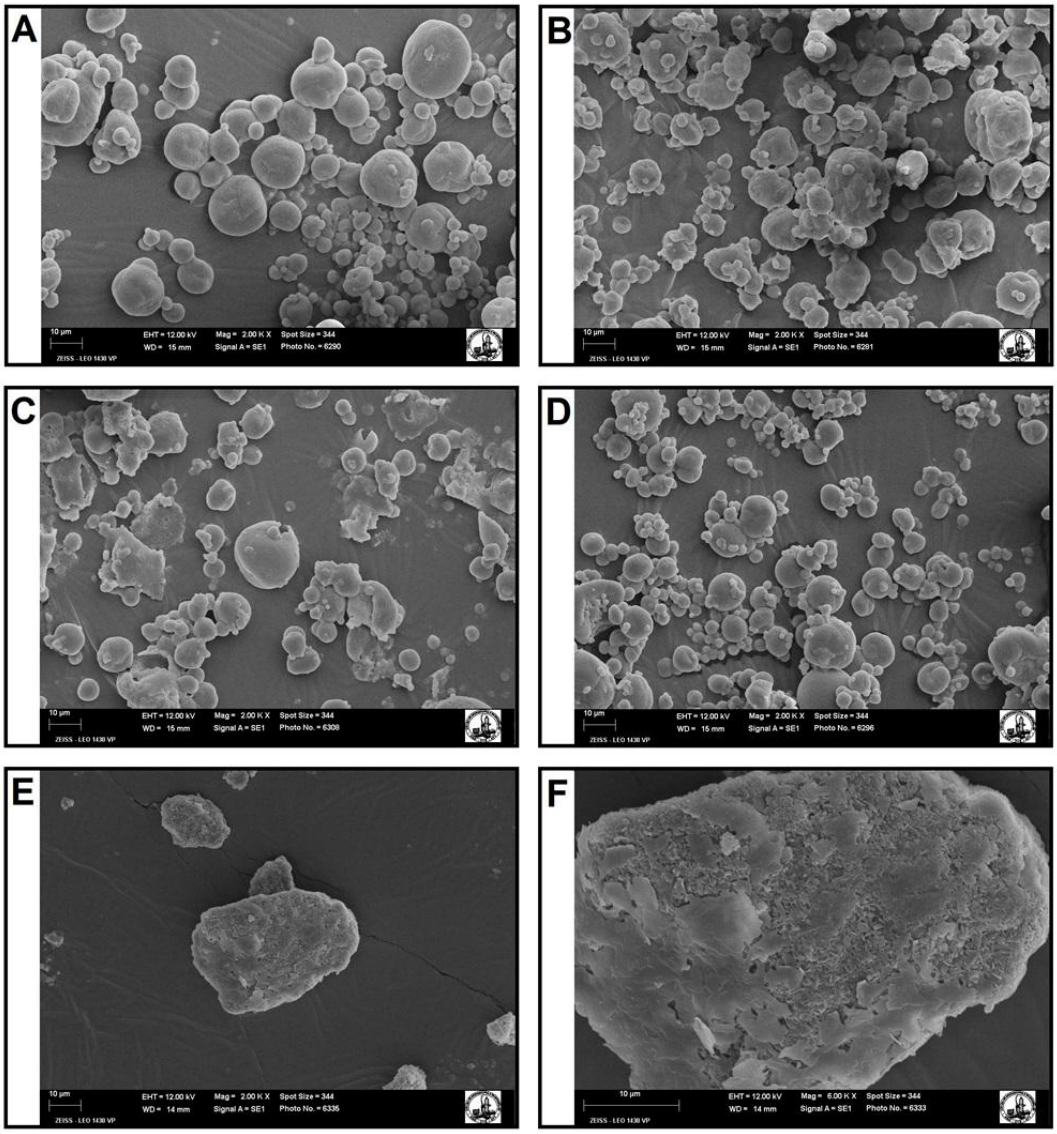


Figure 1. Scanning electron microscopy (SEM) micrographs of AFW-milk powder: (1) Spray-dried powder at: (A) 130°C/0.2 kg/h – 2000×; (B) 130°C/0.8 kg/h – 2000×; (C) 180°C/0.2 kg/h – 2000×; and (D) 180°C/0.8 kg/h – 2000×. (2) Freeze-dried powder at (E) 2000×; FD powder morphology: irregular and angular particles with a rough and porous surface. (F) 6000×; FD powder morphology: evidence of microporosity and fissures. Scale bars = 10 μm.

Among the SD treatments, the 180°C condition produced lower bulk (0.24 ± 0.04 g/mL) and tapped (0.30 ± 0.05 g/mL) densities than the 130°C condition (0.35 ± 0.03 g/mL and 0.44 ± 0.04 g/mL, respectively). This behaviour may be attributed to the formation of more expanded, hollow particles caused by rapid water evaporation and the development of a rigid crust that traps air (Felfoul et al., 2022), making the particles less dense and more prone to cohesion.

Feed rate also affected flow properties at both inlet air temperatures. A feed rate of 0.8 kg/h produced lower Carr index values than 0.2 kg/h, indicating better flowability. This improvement may reflect more uniform particles with lower fines content, since the shorter residence time reduces overdrying and sticky fines formation. However, the relationship between feed rate and fines was not identical at both temperatures, so this effect should be interpreted cautiously. It was observed that at 130°C, increasing the feed rate (0.2 to 0.8 kg/h) reduced the Span [(1.538 ± 0.19) to (0.827 ± 0.11)] and increased the d[0.1] [(0.204 ± 0.030) to (0.451 ± 0.090) μm]. At 180 °C, the Span also decreased [(0.670 ± 0.0800) to (0.632 ± 0.070)], but the d[0.1] dropped [(0.698 ± 0.170) to (0.415 ± 0.070) μm], indicating that the relationship between flow rate and fines is more complex at this temperature.

The influence of drying treatments on density and flow properties is consistent with previous results obtained for spray-dried dairy powders (Felfoul et al., 2022). As Juarez-Enriquez et al. (2022) describe, the high hygroscopicity of FD powder promotes water vapor adsorption and the formation of liquid bridges between particles; under the immediate evaluation conditions, its flowability remained excellent. These literature findings suggest that prolonged storage or exposure to high humidity could compromise the long-term flow behavior of FD powder, which merits investigation in future stability studies.

3.5 Morphological characterization of AFW-milk powders

3.5.1 Particle size distribution

In d[0.5], the 180 °C/0.8 kg/h condition (d[0.5] = 0.690 ± 0.060 μm) did not differ significantly from 130 °C/0.2 kg/h (d[0.5] = 0.584 ± 0.090 μm) and 130°C/0.8 kg/h (d[0.5] = = 0.624 ± 0.090 μm). This suggests that the lower feed flow rate of 180 °C/0.2 kg/h (d[0.5] = 0.941 ± 0.040 μm) may intensify the effect of inlet air temperature on particle size, attributed to thermal expansion and conditions favoring agglomerate formation (Felfoul et al., 2022; Keshani et al., 2015). According to Keshani et al. (2015), lower feed flow rates can increase particle residence time and promote powder deposition, whereas higher feed rates tend to improve process efficiency and reduce chamber retention.

By contrast, the coarse fraction for d[0.9] showed clearer separation: FD (d[0.9] = 2.085 ± 0.150 μm) > 180 °C/0.2 kg/h (d[0.9] = 1.329 ± 0.050 μm) > 180 °C/0.8 kg/h (d[0.9] =

0.851 ± 0.060 μm), indicating that higher feed rate exerts greater shear and reduced thermally formed agglomerates. The highest Span occurred in the FD powder (1.720 ± 0.10), reflecting its irregular, porous structure (Deshwal et al., 2020; Zhou et al., 2025), whereas the Span of SD powders at 180 °C/0.8 kg/h (0.632 ± 0.07) and 180 °C/0.2 kg/h (0.670 ± 0.08) showed narrower distributions consistent with spherical morphology (Figure 1). Narrower particle sizes of SD distributions reflect controlled droplet formation during atomization, whereas freeze-drying produces more heterogeneous particles (Paula et al., 2023).

The finest fraction was characterized by d[0.1] of 0.698 ± 0.17 μm for 180 °C/0.2 kg/h compared to other conditions (Table 2). A higher d[0.1] indicates a coarser fines tail, i.e., a reduced population of very small particles. This behavior suggests that higher inlet air temperature, combined with a lower feed flow rate, shifted fine particles toward larger diameters through coalescence/aggregation, as lower shear allowed agglomerates to remain intact (Felfoul et al., 2022; Keshani et al., 2015). These results are consistent with previous reports (Nugroho et al., 2021; Paula et al., 2023; Zhou et al., 2025).

Particle size is related to the techno-functional characteristics of AFW milk powder. Larger FD particles were associated with higher wettability (37.20 ± 6.72 min) and better flowability (Carr index = 9.28 ± 0.59%), despite higher hygroscopicity and water activity (Deshwal et al., 2020). Conversely, smaller, spherical SD particles, particularly at 180 °C, exhibited lower wettability (at 0.2 kg/h of 426.57 ± 63.27; at 0.8 kg/h of 325.00 ± 15.87), linked to a dense surface and hydrophobic fat barriers (Kim et al., 2002; Nugroho et al., 2021).

Therefore, the drying method and its parameters directly influence particle size distribution and, consequently, powder functionality and process efficiency. Freeze-drying yielded larger particles with superior reconstitution but lower stability, whereas spray-drying resulted in narrower distributions and better stability, highlighting the trade-off between functionality and stability in AFW milk powder production.

3.5.2 Surface topography

Scanning electron microscopy (SEM) was used to compare powder morphology (Figure 1). The freeze-dried (FD) powder consisted of irregular, angular particles with a rough, microporous surface (Figure 1-A, 1-D), a characteristic typical of ice sublimation

from the frozen matrix. This porous structure is consistent with the powder's faster wettability (37.20 ± 6.72 min), resulting from capillary water penetration, as well as its higher hygroscopicity (56.62 ± 4.69%) and water activity (0.626 ± 0.07).

Moisture absorption promotes plasticization of the amorphous matrix (Li et al., 2016) and is expected to lower the glass transition temperature (Tg), shifting the material from the glassy to the rubbery state (Jouppila & Roos, 1994). This mechanism is proposed as a literature-based interpretation of the observed behavior. The higher molecular mobility in the rubbery state may have contributed to the higher browning index observed in the FD powder (39.72 ± 4.53), suggesting a greater extent of non-enzymatic browning, potentially associated with Maillard reactions. Thus, browning may be linked to cryoconcentration, residual moisture, and increased molecular mobility. Because the browning mechanism was not directly measured, this interpretation should be read as a hypothesis rather than a confirmed mechanism.

In contrast, the SD powders consisted of spherical particles with surfaces ranging from smooth to moderately rough (Figures 1B, 1C). Their lower hygroscopicity compared with the FD powder (56.62 ± 4.69%) is consistent with several possible factors, such as those discussed in Section 3.3: lactose crystallization favored by high inlet air temperatures (130–180 °C) (Jouppila & Roos, 1994); dense, spherical morphology with lower specific surface area (Zhou et al., 2025); surface enrichment in fat and partially crystalline lactose that may form a hydrophobic barrier (Kim et al., 2002; Zouari et al., 2020); and lower residual moisture (0.68 ± 0.20%–1.35 ± 1.01%) and water activity (0.160 ± 0.02–0.261 ± 0.02), which are expected to increase glass transition temperature (Tg) and reduced molecular mobility (Li et al., 2016; Pugliese et al., 2018). These factors are consistent with the lower hygroscopicity and greater stability of the SD powders under humid conditions. These mechanisms are compatible with the observed results, but direct measurements of lactose crystallinity, Tg, and surface composition would be needed to confirm them.

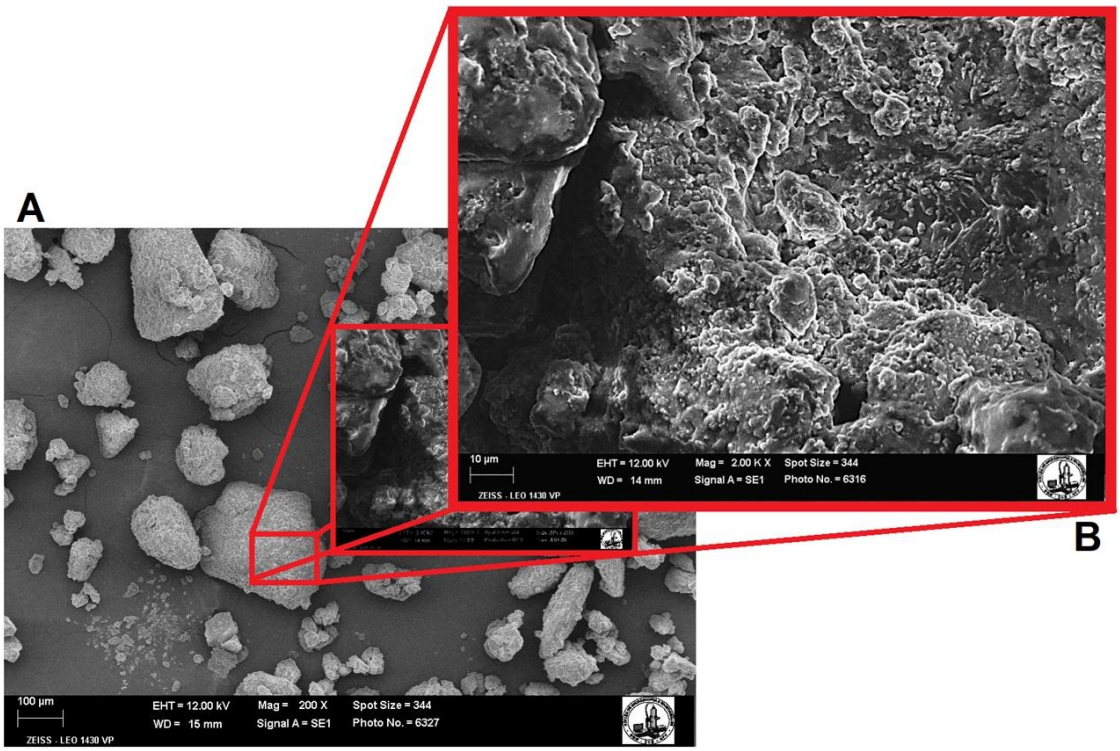


Figure 2. Scanning electron microscopy (SEM) micrographs of freeze-dried AFW-milk powder at different magnifications. (A) 200×; powder morphology: irregular and angular particles with a heterogeneous size distribution; red square: region selected for analysis at higher magnification. (B) 2000× of the surface highlighted in (A); powder morphology: rough, microporous, and fissured surface (typical image of ice sublimation from a frozen matrix). Scale bars: 100 µm (A) and 10 µm (B).

Higher-magnification SEM analysis further characterized the freeze-dried powder (Figure 2). At 200× magnification (Figure 2A), the powder showed irregular, angular particles with a heterogeneous size distribution, characteristic of ice sublimation during freeze-drying; the red square indicates the representative particle selected for detailed analysis. At 2000× magnification (Figure 2B), the particle surface revealed a rough, microporous structure with evident fissures. This porous morphology is consistent with selective water freezing during the freezing stage, resulting in a concentrated solute matrix that sublimes under vacuum (Balde & Aïder, 2017) (condenser temperature of -40°C and an operating pressure range of 0.1 to 1.0 mbar for 48 h). These characteristics are consistent with the previously reported wettability, hygroscopicity, and water activity.

3.6 Process efficiency

Drying losses compromise process performance by reducing productivity and increasing product degradation, cleaning downtime, and operational safety risks, while also lowering final product quality (Ramírez-Rivera et al., 2025). Total losses and powder retention within the drying chamber were evaluated to determine operational efficiency. Losses during spray drying (SD) were significantly lower ($p < 0.05$) than those observed in freeze-drying (FD) (Table 2).

Total losses for spray-dried powders were strongly influenced by inlet air temperature: all treatments at 130°C showed the lowest losses, with no effect of feed flow rate, whereas treatments at 180°C and FD did not differ statistically ($p < 0.05$) and showed higher losses.

Powder retention on the drying chamber walls (Table 2) is a key spray-drying parameter. High retention values indicate that a significant portion of the product adheres to the equipment and is not recovered in the main cyclone. Wall deposition is common with highly adhesive products or those containing thermoplastic components, such as milk powder, and can reduce collection efficiency while increasing cleaning downtime. Adjusting the outlet air temperature or employing auxiliary stages (e.g., a fluidized bed or air-sweeping system) can mitigate this retention (Ahmed et al., 2024; Keshani et al., 2015; Moradi Maryamnegari et al., 2022).

For the temperatures evaluated (130 and 180 °C, respectively), retention in the chamber at 0.2 kg/h (53.63 ± 0.63% and 54.77 ± 2.09%) was higher than that observed at 0.8 kg/h (38.25 ± 3.26% and 42.99 ± 0.91%). This result suggests that the lower feed flow favors deposition under the conditions evaluated. However, particle size alone does not explain this behavior. It may reflect a combination of operational and surface factors: finer particles may be preferentially entrained and deposited on the walls, since the 0.2 kg/h treatment produced larger, more agglomerated particles rather than a finer population. Possible explanations include: (i) longer residence time of particles in the chamber, increasing the probability of collision with the walls; (ii) greater surface humidity and cohesiveness of larger particles formed at low flow rates, favoring adhesion; and (iii) partial agglomeration, which can generate particles with an irregular surface and a larger effective contact area (Keshani et al., 2015; Ramírez-Rivera et al., 2025). The higher retention at 0.2 kg/h was observed despite larger particles, suggesting that

factors other than particle size likely contributed, including a combination of factors: longer particle residence time in the chamber (operational), higher surface moisture and cohesiveness of larger particles, and partial agglomeration (surface), which require further investigation.

Process efficiency is also related to the techno-functional characteristics of the powders. The higher retention in the chamber observed at a feed rate of 0.2 kg/h (at 130 °C of 53.63 ± 0.63% and at 180 °C of 54.77 ± 2.09%) compared to 0.8 kg/h (at 130 °C of 38.25 ± 3.26% and at 180 °C of 42.99 ± 0.91%) cannot be attributed simply to a higher proportion of fine particles, since particle size data show that at 0.2 kg/h, the particles were larger and had a lower fines content (d[0.1] = 0.698 ± 0.17 μm at 180 °C/0.2 kg/h vs. 0.415 ± 0.07 μm at 180 °C/0.8 kg/h). This apparent paradox suggests that other mechanisms govern retention, such as the longer residence time of particles in the chamber at low feed rates, increasing the probability of wall collisions, and the higher surface moisture and cohesiveness of larger particles, which favor adhesion (Keshani et al., 2015; Ramírez-Rivera et al., 2025). Thus, the high retention at 0.2 kg/h likely results from a combination of operational and surface factors, rather than particle size alone. Higher chamber retention at low feed rate may reflect residence time, surface moisture, cohesiveness, and partial agglomeration.

4. CONCLUSIONS

Spray drying and freeze-drying produced additive-free, pasteurized, homogenized whole milk powders with distinct physicochemical, color, techno-functional, flow, morphological, and process-efficiency profiles. Spray drying generally yielded spherical, denser powders with lower water activity, lower hygroscopicity, narrower particle-size distributions, and lower drying losses than freeze-drying, indicating greater storage stability. In contrast, freeze-drying produced irregular, porous particles with better wettability and flowability, but also higher water activity, hygroscopicity, browning index, and drying losses, suggesting lower physicochemical stability under the conditions evaluated. Among the spray-drying conditions tested, 130 °C and 0.8 kg/h suggested the most balanced performance in physicochemical stability and process efficiency, although the higher moisture variability at this condition indicates that additional replicates would be needed to confirm reproducibility. Although 180 °C and 0.8 kg/h produced a narrower particle-size distribution and lower moisture, it also worsened wettability and increased mass losses, so it cannot be considered universally superior.

Because this was a bench-scale study, pilot-scale validation is still required before industrial application. Future work should confirm the proposed browning mechanisms with Maillard markers and, where feasible, include measurements of glass transition temperature and surface composition.

AUTHOR CONTRIBUTIONS

Jhonatan Faria da Costa: data curation, formal analysis, investigation, methodology, supervision, writing-original draft. José Roberto Miranda Júnior: supervision; writing-review and editing. Bruna Mara Aparecida de Carvalho Mesquita: supervision; writing-review and editing. Moysés Naves de Moraes: supervision; writing-review and editing. César Augusto Sodré da Silva: supervision; writing-review and editing. Jane Sélia dos Reis Coimbra: supervision; writing-review and editing; funding acquisition.

CONFLICTS OF INTEREST

The authors reported no potential conflicts of interest.

ACKNOWLEDGMENTS

The authors thank the Instituto Federal do Sudeste de Minas Gerais (IF Sudeste MG) for its institutional support.

FUNDING

This study received financial support from the Coordenação de Aperfeiçoamento de Pessoal de Nível Superior (CAPES) (Funding Code 001), Conselho Nacional de Desenvolvimento Científico e Tecnológico (CNPq), Financiadora de Estudos e Projetos (FINEP), Fundação de Amparo à Pesquisa do Estado de Minas Gerais (FAPEMIG) (APQ-00784-23), Núcleo de Microscopia e Microanálise (NMM/UFV), and the Laboratório de Nanomateriais e Química Ambiental (LANAQUA/UFV).

REFERENCES

AHMED, M. W.; SCHULNIES, F.; KLEINSCHMIDT, T. Residence time distribution and kinetics of insolubility of skim milk powder during spray drying. Food and Humanity, 2, 2024.

AOAC. Official methods of analysis of the Association of Official Analytical Chemists. Association of Official Analytical Chemists International, Gaithersburg, Rockville, MD, USA, 2016.

BALDE, A.; AÏDER, M. Effect of cryoconcentration, reverse osmosis and vacuum evaporation as concentration step of skim milk prior to drying on the powder properties. Powder Technology, 319, p. 463-471, 2017.

BHANDARI, B.; BANSAL, N.; ZHANG, M.; SCHUCK, P. Handbook of Food Powders: Chemistry and Technology. Second Edition. 2023. 978-0-323-98820-9.

BRAGA, M. B.; VEGGI, P. C.; CODOLO, M. C.; GIACONIA, M. A. et al. Evaluation of freeze-dried milk-blackberry pulp mixture: Influence of adjuvants over the physical properties of the powder, anthocyanin content and antioxidant activity. Food Research International, 125, p. 108557, Nov 2019.

DESHWAL, G. K.; SINGH, A. K.; KUMAR, D.; SHARMA, H. Effect of spray and freeze drying on physico-chemical, functional, moisture sorption and morphological characteristics of camel milk powder. LWT - Food Science and Technology, 134, p. 110117, 2020.

FARAG, M. A.; KHALIFA, I.; GAMAL, M.; BAKRY, I. A. The chemical composition, production technology, authentication, and QC analysis of dried milk. International Dairy Journal, 133, 2022.

FELFOUL, I.; BURGAIN, J.; PERROUD, C.; GAIANI, C. et al. Impact of spray-drying conditions on physicochemical properties and rehydration ability of skim dromedary and cow's milk powders. Drying Technology, 40, n. 3, p. 665-677, 2022.

FIALHO, T. L.; MARTINS, E.; SILVA, C. R. D. J.; STEPHANI, R. et al. Lactose-hydrolyzed milk powder: Physicochemical and technofunctional characterization. Drying Technology, 36, n. 14, p. 1688-1695, 2018.

FOURNAISE, T.; BURGAIN, J.; PERROUD, C.; SCHER, J. et al. Impact of formulation on reconstitution and flowability of spray-dried milk powders. Powder Technology, 372, p. 107-116, 2020.

GAIANI, C.; SCHUCK, P.; SCHER, J.; DESOBRY, S. et al. Dairy powder rehydration: influence of protein state, incorporation mode, and agglomeration. Journal of Dairy Science, 90, n. 2, p. 570-581, 2007.

HAMEDI, S.; AFSAHI, M. M.; NEMATOLLAHI, M. H.; AKHAVAN, H. R. Spouted bed drying of skimmed milk: Multivariable optimization of the conditions to improve physicochemical properties of the dried milk. LWT - Food Science and Technology, 146, 2021.

ISO. Dried milk and milk products, Determination of insolubility Index, ISO 8156:2005 / IDF 129:2005. 2005.

ISO. Instant dried milk, Determination of the dispersibility and wettability, ISO/TS17758/IDF/RM 87:2014. 2014.

JI, J.; FITZPATRICK, J.; CRONIN, K.; MAGUIRE, P. et al. Rehydration behaviours of high protein dairy powders: The influence of agglomeration on wettability, dispersibility and solubility. Food Hydrocolloids, 58, p. 194-203, 2016.

JOUPPILA, K.; ROOS, Y. H. Glass Transitions and Crystallization in Milk Powders. Journal of Dairy Science, 77, n. 10, p. 2907-2915, 1994.

JUAREZ-ENRIQUEZ, E.; OLIVAS, G. I.; ZAMUDIO-FLORES, P. B.; PEREZ-VEGA, S. et al. A review on the influence of water on food powder flowability. Journal of Food Process Engineering, 45, n. 5, 2022.

KAWASAKI, H.; SHIMANOUCHI, T.; KIMURA, Y. Recent Development of Optimization of Lyophilization Process. Journal of Chemistry, 2019, p. 1-14, 2019.

KESHANI, S.; DAUD, W. R. W.; NOUROUZI, M.; NAMVAR, F. et al. Spray drying: An overview on wall deposition, process and modeling. Journal of Food Engineering, 146, p. 152-162, 2015.

KILIC-AKYILMAZ, M.; OZER, B.; BULAT, T.; TOPCU, A. Effect of heat treatment on micronutrients, fatty acids and some bioactive components of milk. International Dairy Journal, 126, 2022.

KIM, E. H. J.; CHEN, X. D.; PEARCE, D. Surface characterization of four industrial spray-dried dairy powders in relation to chemical composition, structure and wetting property. Colloids and Surfaces B: Biointerfaces, 26, n. 3, p. 197-212, 2002.

LI, R.; ROOS, Y. H.; MIAO, S. The effect of water plasticization and lactose content on flow properties of dairy model solids. Journal of Food Engineering, 170, p. 50-57, 2016.

LIU, Y.; ZHANG, W.; HAN, B.; ZHANG, L. et al. Changes in bioactive milk serum proteins during milk powder processing. Food Chemistry, 314, p. 126177, June 1, 2020.

MOEJES, S. N.; VAN BOXTEL, A. J. B. Energy saving potential of emerging technologies in milk powder production. Trends in Food Science & Technology, 60, p. 31-42, 2017.

MORADI MARYAMNEGARI, S.; ASHRAFIZADEH, A.; JASKULSKI, M. A novel approach for the reduction of powder deposition in spray drying chambers. Drying Technology, 41, n. 6, p. 1017-1030, 2022.

NASSER, S.; MOREAU, A.; JEANTET, R.; HÉDOUX, A. et al. Influence of storage conditions on the functional properties of micellar casein powder. Food and Bioproducts Processing, 106, p. 181-192, 2017.

NUGROHO, R. W. N.; OUTINEN, M.; TOIKKANEN, O.; HEINO, A. et al. Effect of water activity on the functional, colloidal, physical, and microstructural properties of infant formula powder. Journal of Colloid and Interface Science, 586, p. 56-66, March 15, 2021.

NUGROHO, R. W. N.; OUTINEN, M.; TOIKKANEN, O.; ROJAS, O. J. Particle size and fat encapsulation define the colloidal dispersibility and reconstitution of growing-up milk powder. Powder Technology, 391, p. 133-141, 2021.

O'SULLIVAN, J. J.; NORWOOD, E.-A.; O'MAHONY, J. A.; KELLY, A. L. Atomisation technologies used in spray drying in the dairy industry: A review. Journal of Food Engineering, 243, p. 57-69, 2019.

PAULA, I. L.; MELQUÍADES, L. L.; PERRONE, Í. T.; MAURICIO, E. F. et al. Reduced and Low-lactose Powdered Milk Production and Determination of its Physicochemical and Microstructural Properties During Storage. Revista Virtual de Química, 15, n. 5, p. 887-895, 2023.

PHOSANAM, A.; CHANDRAPALA, J.; ZISU, B.; ADHIKARI, B. Storage stability of powdered dairy ingredients: a review. Drying Technology, 39, n. 11, p. 1529-1553, 2021.

PUGLIESE, A.; CABASSI, G.; CHIAVARO, E.; PACIULLI, M. et al. Physical characterization of whole and skim dried milk powders. Journal of Food Science and Technology, 54, n. 11, p. 3433-3442, 2017.

PUGLIESE, A.; PACIULLI, M.; CHIAVARO, E.; MUCCHETTI, G. Application of differential scanning calorimetry to freeze-dried milk and milk fractions. Journal of Thermal Analysis and Calorimetry, 137, n. 2, p. 703-709, 2018.

RAMÍREZ-RIVERA, M. J.; DÍAZ-OVALLE, C. O.; RAMOS-OJEDA, E.; FLORES-GÓMEZ, C. A. An CFD approach to reduce the risk of wall deposition in the milk powder process. Food and Bioproducts Processing, 152, p. 178-190, 2025.

ROOS, Y. H. Glass transition temperature and its relevance in food processing. Annual Review of Food Science and Technology, 1, n. 1, p. 469-496, 2010.

RYABOVA, A. E.; SEMIPYATNY, V. K.; GALSTYAN, A. G. Effects of storage conditions on milk powder properties. Journal of Dairy Science, 106, n. 10, p. 6741-6758, Oct 2023.

SCHUCK, P.; JEANTET, R.; DOLIVET, A. Analytical Methods for Food and Dairy Powders. John Wiley & Sons, 2012. 1118307429.

SHARMA, A.; JANA, A. H.; CHAVAN, R. S. Functionality of Milk Powders and Milk-Based Powders for End Use Applications—A Review. Comprehensive Reviews in Food Science and Food Safety, 11, n. 5, p. 518-528, 2012.

SUESS, E. Robust multiparameter analysis of infant and follow-on formulas with ion chromatography (IC). White Paper (WP-077). Herisau: Metrohm, 2021. Disponível em: https://www.metrohm.com/content/dam/metrohm/shared/documents/white-papers/WP-077EN.pdf.

WU, W. D.; LIU, W.; GENGENBACH, T.; WOO, M. W. et al. Towards spray drying of high solids dairy liquid: Effects of feed solid content on particle structure and functionality. Journal of Food Engineering, 123, p. 130-135, 2014.

ZAFISAH, N. S.; YUSOF, Y. A.; ALI, M. A.; ROSLAN, N. S. et al. Processing of raw coconut milk for its value addition using spray and freeze drying techniques. Journal of Food Process Engineering, 41, n. 1, 2017.

ZHOU, S.; ZHANG, X.; ZHANG, J.; ZANG, C. et al. Differences in physicochemical properties and proteomics analysis of spray-and freeze-dried milk powders from bovine, goat, and horse sources. Journal of Dairy Science, 108, n. 2, p. 1367-1379, 2025.

ZOUARI, A.; SCHUCK, P.; GAUCHERON, F.; TRIKI, M. et al. Microstructure and chemical composition of camel and cow milk powders' surface. LWT - Food Science and Technology, 117, p. 108693, 2020.